Experimental and theoretical investigation of two-cell stimulated-Brillouin-scattering systems

G. J. Crofts and M. J. Damzen

Laser Optics Section, Blackett Laboratory, Imperial College, Prince Consort Road, London SW7 2BZ, UK

R. A. Lamb

Defence Research Agency, Military Division, RARDE, Fort Halstead, Sevenoaks, Kent TN14 7BP, UK

Received February 26, 1991; revised manuscript received June 17, 1991

The use of a two-cell stimulated-Brillouin-scattering (SBS) system to extend the dynamic-power range of a phase-conjugate mirror is investigated experimentally and theoretically. A pulsed, frequency-doubled Nd:YAG laser system is used to study the SBS generator–amplifier arrangement, and the results demonstrate an increase in the achievable efficiency and dynamic-power range of the SBS mirror compared with a single-cell system while maintaining good phase-conjugate fidelity for a near-diffraction-limited beam. A full transient numerical modeling of the system is also presented, together with steady-state calculations for comparison. The technique of generator–amplifier geometries is applicable to other forms of stimulated scattering, including stimulated photorefractive scattering.

INTRODUCTION

Stimulated Brillouin scattering (SBS) is widely used as a convenient method for phase conjugating pulsed laser radiation. The process can be efficient at moderate powers (a few megawatts), and high-fidelity phase conjugation can be achieved using a focused geometry or by propagating through a waveguide containing a Brillouin active medium. At higher laser powers the onset of competing nonlinearities such as optical breakdown, thermal heating, and self-focusing can completely disrupt the SBS process, reducing efficiency and phase-conjugate fidelity. The problem of high intensity can be overcome by scaling to larger-aperture geometries, but the phase-conjugate fidelity is severely degraded owing to the increased number of uncorrelated Stokes modes that are then amplified.[1]

A simple method for extending the dynamic-power range of the SBS mirror is by using a two-cell SBS system. A schematic of the two-cell configuration is shown in Fig. 1. The arrangement consists of a large-aperture front cell (SBS amplifier) that receives the full incident power (P_a) in series with a small-aperture back cell (SBS generator) that receives a fraction of the incident power (P_g) owing to pump depletion in the SBS amplifier and any intercell attenuation. The generator cell can be arranged in a geometry appropriate for obtaining high-fidelity phase conjugation, such as one that uses a small-diameter waveguide or tight focusing. In this configuration the amplifier cell is seeded by a phase-conjugate Stokes beam (P_g^*) rather than being initiated from spontaneous noise. Since the conjugate selectivity of the large-aperture amplifier is poor, the presence of a relatively strong conjugate seed signal is expected to improve greatly the fidelity of this geometry.[1] Indeed several authors have reported efficient phase conjugation of high-power, near-diffraction-limited laser radiation using the generator–amplifier scheme.[2-7] The technique of backseeding a phase-conjugate mirror has also been used with photorefractive crystal barium titanate ($BaTiO_3$) where the seed signal was provided by a retroreflecting pseudoconjugator.[8]

This paper presents experimental investigations of a SBS generator–amplifier arrangement using a pulsed, frequency-doubled Nd:YAG laser system. The efficiency of the two-cell system is studied together with the temporal evolution of the pump and Stokes radiation in the system. Results of numerical modeling to simulate the transient SBS process are presented along with steady-state calculations, which are expected to provide qualitative trends to the behavior of the two-cell system.[9] Finally a discussion of the results is made and conclusions presented.

EXPERIMENTAL

The experimental arrangement is shown in Fig. 2. Laser radiation was provided by the frequency-doubled (532 nm), Q-switched output from a Nd:YAG oscillator and amplifier chain operating on a single-longitudinal and single-transverse model (TEM_{00}). The pulse energy could be varied up to a maximum of approximately 100 mJ with a pulse duration of approximately 12 ns FWHM. Temporal data were recorded using photodiodes with a rise time of 125 ps and transient digitizers with a bandwidth of 250 MHz. The SBS generator–amplifier system shown in Fig. 2 consists of two cells arranged in a series, each preceded by a converging lens. The pump radiation enters the system through a long-focal-length lens (f = 2.2 m) situated 1.6 m from the entrance window of the amplifier cell. This arrangement provides soft focusing of the pump radiation and allows control of the intensity of the pump radiation in the amplifier cell by the lens-to-cell separation. A more powerful lens (f = 10 cm) then focuses the beam into the generator cell. The separation between the back of the amplifier cell and the front of the

0740-3224/91/112282-07$05.00

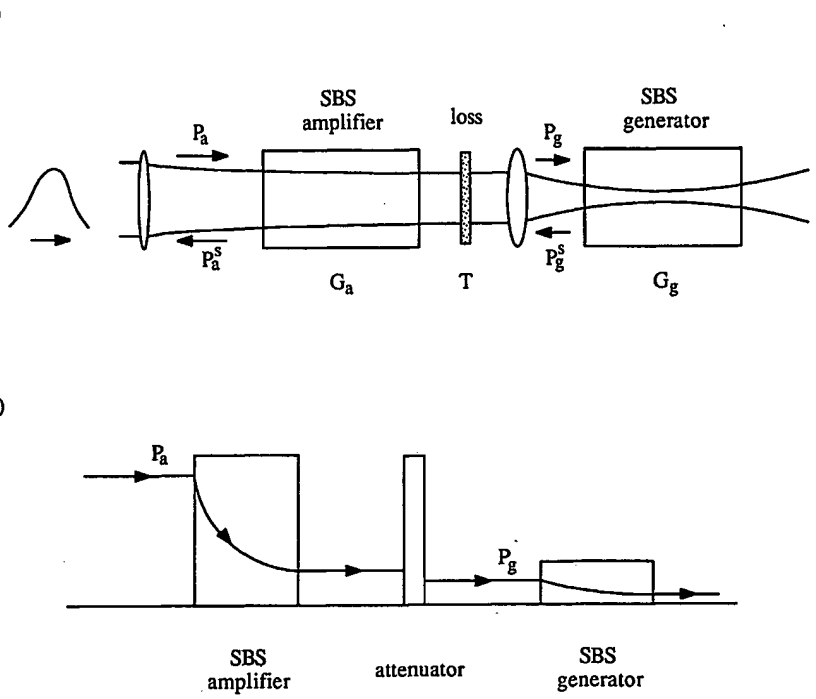

Fig. 1. (a) Two-cell SBS system. .(b) Schematic diagram of laser pump power distribution in the two-cell system.

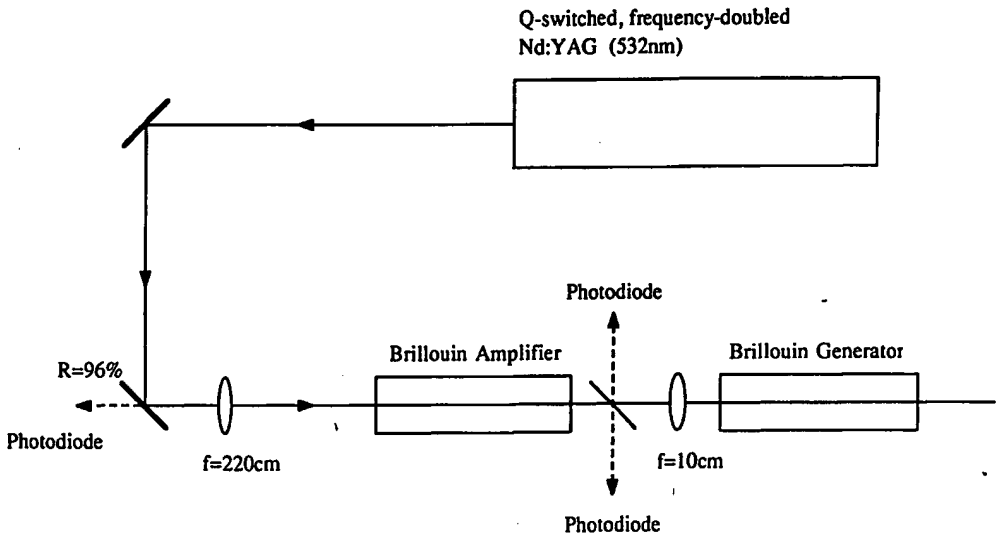

Fig. 2. Experimental arrangement for studying the two-cell geometry.

generator cell was 25 cm. The Brillouin active medium used was acetone. The generator cell length was 19 cm, and six different amplifier-cell lengths between 2 and 30.5 cm were investigated.

The presence of the amplifier cell suppressed the problem of breakdown up to the maximum available laser energy of 100 mJ. Consequently, as the curves of Fig. 3 show, greater energy reflectivities have been achieved by using a two-cell system (96%) than by using a focused single-cell system (90%). The performance of the system can also be characterized by an energy-amplification factor defined as the ratio of the total-output Stokes energy from the two-cell system of the Stokes seed energy entering the SBS amplifier from the generator cell. Figure 4 shows the amplification (A) measured experimentally for different cell lengths with the input-pump energy normalized to the observational-threshold energy for SBS to occur in the amplifier cell alone. The data demonstrate a smooth trend toward greater amplification at higher pump energies. As expected, the threshold energy of the amplifier equated to the usual exponential-gain coefficient (gIL) of approximately 25–30. Measurements showed that the threshold energy varied in a predictable manner if the position of the amplifier cell in the converging beam was adjusted or the cell length was changed. This is corroborated by the fact that in Fig. 4 all the data points lie on a smooth curve even though different amplifier-cell lengths were used. This is because

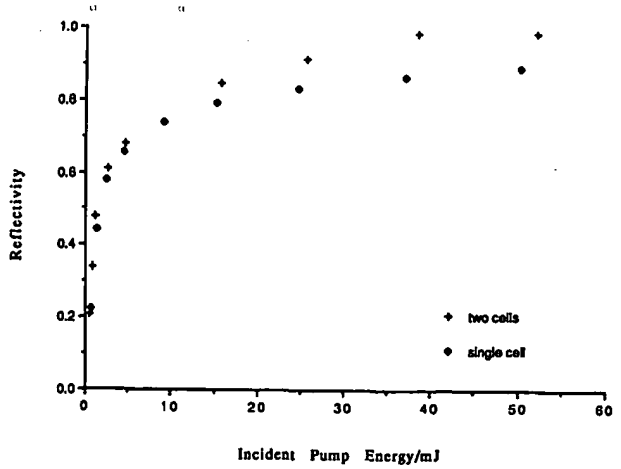

Fig. 3. Experimental energy reflectivity (R) for the two-cell system and for a single cell against input-pulse energy.

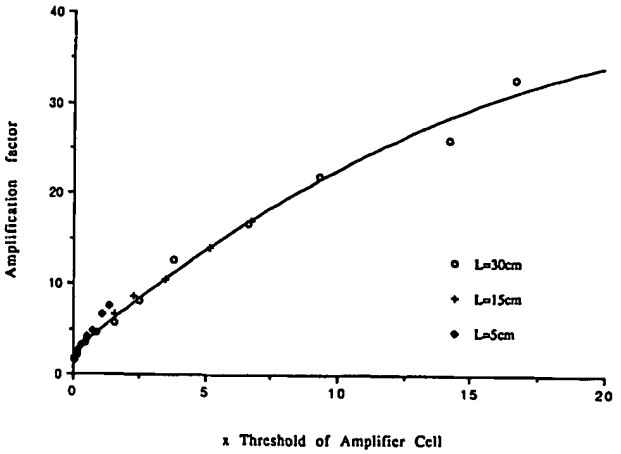

Fig. 4. Experimental amplification factor (A) for different amplifier-cell lengths contrasted against input-pulse energy normalized to the threshold energy of the amplifier cell.

the input pump energies are normalized to the threshold energy of the amplifier, which changes for different cell lengths to maintain a threshold small-signal gain of 25–30.

Further insight into the operation of the two-cell system can be gained by monitoring the temporal evolution of the intercell radiation. An example of the typical behavior observed for a temporally Gaussian input pulse is shown in Fig. 5. At higher powers the seed pulse (P_g^s) displays some modulation [Fig. 5(b)] that was also present on the incoming intercell pump pulse (P_g). This is owing to the sensitive dependence of radiation transmitted through the amplifier on small changes in reflectivity when the amplifier is operated in a highly saturated regime. The transmitted radiation and subsequent seed signal grow and decay periodically as a result of the acoustic response and intercell round-trip times. This behavior is analogous to the relaxation oscillation characteristic of some laser systems. The dependence of the modulation period on the round-trip time was verified experimentally by varying the cell separation. It was found that as the cell separation was increased the modulation period was observed to increase by an amount greater than the increment in intercell round-trip time. This confirms that the modulation period is not merely dependent on the intercell round-trip time but is also a function of the decay and buildup of the acoustic waves in both the generator and amplifier cells. In contrast, the total transmitted Stokes signal (P_a^s) of Fig. 5(a) displays little modulation. The oscillatory temporal features of the seed signal are smoothed out owing to the strong saturation of the Brillouin amplifier. The output Stokes signal was relatively smooth for all amplifier-cell lengths tested. At low input energies and short amplifier-cell lengths, the gain of the amplifier is low and thus does not significantly contribute to the interaction. In this regime the two-cell system reverts to single-cell behavior and yields smooth output pulses.

The phase-conjugate fidelity of the backscattered radiation is also of interest. The phase-conjugate fidelity of the two-cell system was clearly better than for the large-aperture amplifier alone, which when unseeded did not produce a conjugate but rather a noisy speckle pattern.[2] The presence of a seed signal that is well correlated with the input Gaussian beam results in greater discrimination in the amplifier against nonconjugate light distributions. In the experiments it was found that with all the pump energies investigated the two-cell system produced a high-quality Stokes output in which virtually all the energy was contained within a low-divergence beam. Consequently the output radiation displayed a high fidelity similar to that measured for a single cell in a focused geometry.[10] This indicates that the presence of the amplifier does not noticeably degrade the phase conjugation of high-quality radiation. Indeed, since the presence of the amplifier suppressed the optical breakdown in the generator

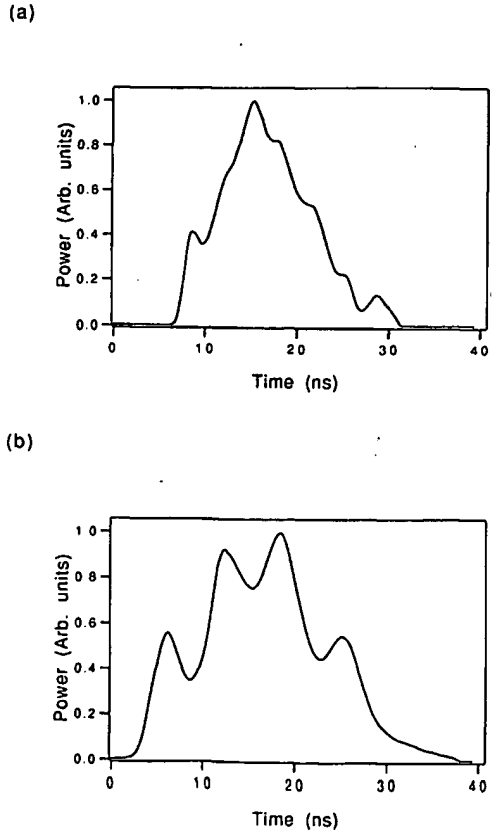

Fig. 5. Experimental temporal profiles for (a) total reflected Stokes signal and (b) intercell Stokes seed signal.

cell, the result was that the two-cell system exhibited superior phase conjugation at input energies well in excess of the SBS threshold. This result derives from the power-limiting behavior of the amplifier. This behavior protects the generator and is analogous to the situation discussed by Bubis *et al.*[10] of SBS in a focal constriction in which the prefocal region screens the focus.

THEORETICAL PREDICTIONS

In order to compare the experimental situation with theory, the transient equations describing the SBS process in the amplifier and generator cells are modeled numerically. The evolution of the amplifier (generator) pump field E_a (E_g), Stokes field S_a (S_g), and acoustic-wave amplitude Q_a (Q_g) are described by the following system of equations:

$$\left(\frac{\partial}{\partial z}+\frac{n}{c}\frac{\partial}{\partial t}\right)E_{a,g}=-\frac{g}{2}\Gamma S_{a,g}Q_{a,g}, \tag{1a}$$

$$\left(\frac{\partial}{\partial z}-\frac{n}{c}\frac{\partial}{\partial t}\right)S_{a,g}=-\frac{g}{2}\Gamma E_{a,g}Q_{a,g}^{*}, \tag{1b}$$

$$\frac{\partial Q_{a,g}}{\partial t}=E_{a,g}S_{a,g}^{*}-\Gamma Q_{a,g}, \tag{1c}$$

where c/n is the speed of light in the medium, g is the steady-state Brillouin gain coefficient, and Γ is the Brillouin linewidth. Plane waves are assumed in the simulation, but the noncollimated geometry is accounted for by allowing an area variation $A_{a,g}(z)$ which, together with the laser power in the two cells $P_{a,g}$, determines the intensity $I_{a,g}$:

$$I_{a,g}(z,t)=\frac{P_{a,g}(z,t)}{A_{a,g}(z)}=|E_{a,g}(z,t)|^{2}. \tag{2}$$

The boundary conditions appropriate to the two-cell system are

$$P_g(0,t)=TP_a(L_a,t-\tau), \tag{3a}$$

$$P_a^{s}(L_a,t)=TP_g^{s}(0,t-\tau), \tag{3b}$$

for laser powers $P_{a,g}$ and Stokes powers $P_{a,g}^{s}$ where T is the intercell transmission factor and τ is the intercell time of flight. The input-pump beam to the amplifier [$P_a(0,t)$] is specified as a Gaussian pulse, and the SBS interaction in the generator is initiated by the usual spontaneous noise level $|S_g(L_g,t)|^2 \simeq |E_g(L_g,t)|^2 \exp(-D)$, where typically D has a value of approximately 30.

In the tightly focused geometry of the generator cell, propagation effects owing to the transit time through the cell can be neglected, and the equations are transformed to permit more accurate modeling and greater numerical stability, particularly at high pump intensities (see Appendix A).

For the sake of generality, the pump and Stokes powers calculated in the simulation are normalized to the cell lengths ($L_{a,g}$) and area variations [$A_{a,g}(z)$] in the form of a small-signal gain, as has been done before.[6] The input-pump gains are given by

$$G_a(t)=gP_a(0,t)\int_0^{L_a}\frac{dz}{A_a(z)}, \tag{4a}$$

$$G_g^{D}(t)=gP_g(0,t)\int_0^{L_g}\frac{dz}{A_g(z)}, \tag{4b}$$

where G_a is the small-signal input to the amplifier and G_g^{D} is the small-signal input to the generator after depletion by the amplifier. The output Stokes gains are similarly defined.

Figure 6 shows the results of a typical simulation for a 25-mJ pulse of duration 11.6 ns incident on a 20-cm amplifier cell containing acetone [$g \approx 0.0158$ cm/MW and $1/\Gamma \approx 0.76$ ns (from Ref. 11)]. The output Stokes beam of Fig. 6(a) closely follows the pump beam, displaying a high reflectivity with only a small amount of modulation. The intercell pump and Stokes radiation of Fig. 6(b) are characterized by a high degree of modulation owing to reasons discussed above. The temporal forms of the pump input and Stokes output from the amplifier and generator cells are reproduced in Fig. 7 with a steady-state calculation superimposed. As anticipated[9] the steady-state model gives a qualitative guide to the average behavior of the whole system [Fig. 7(b)]. However, the steady-state behavior of the intercell radiation rapidly deviates from the average of the transient behavior as the input energy is increased. This is a result of lower transmission through the amplifier under steady-state conditions and subsequent lower levels of intercell radiation. The transient and steady-state energy reflectivity (R) and amplification factors (A) have also been calculated and are plotted against pulse energy in Fig. 8. The steady-state energy amplification (A) is readily deduced from an earlier analysis[6] and is given by

$$A=\frac{R(1-T^{2}R_g)}{T^{2}R_g(1-R)}, \tag{5}$$

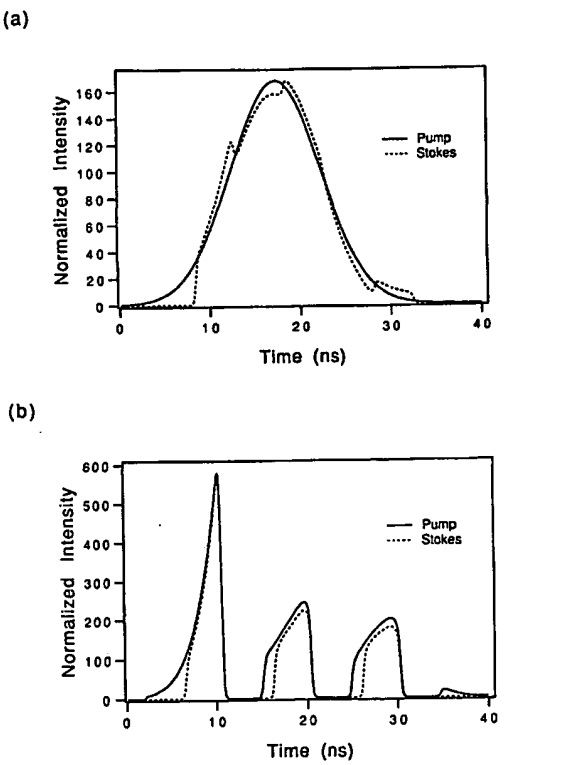

Fig. 6. Numerical simulations of the pump and Stokes temporal profiles for (a) amplifier and (b) generator.

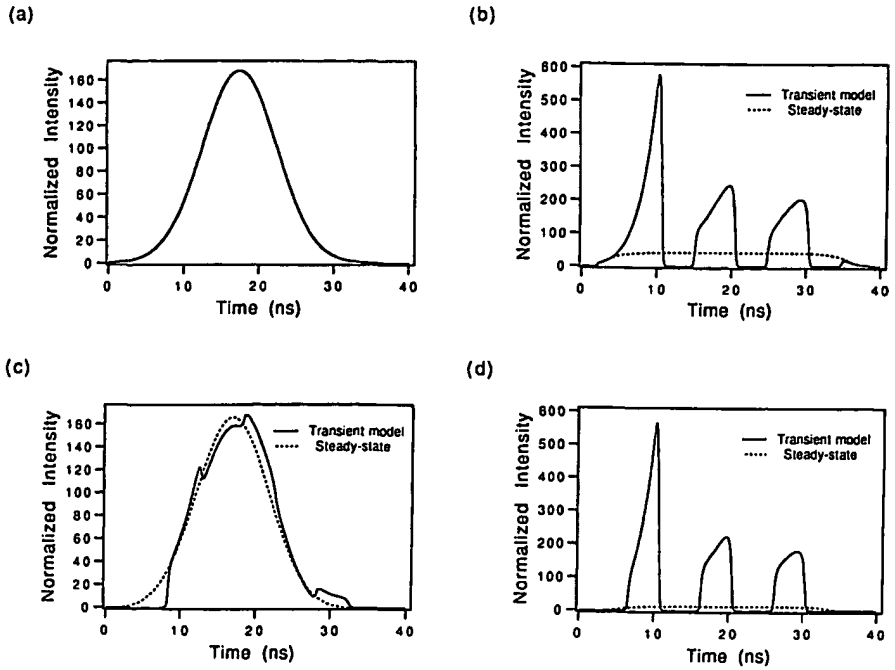

Fig. 7. Numerical simulation and steady-state calculation of the evolution of the pump radiation into (a) the amplifier and (b) the generator and of the Stokes radiation out of (c) the amplifier and (d) the generator.

where R_g is the steady-state SBS reflectivity of the generator cell. As can be seen in Fig. 8(b), the steady-state behavior of the amplification deviates from the transient model owing to its sensitive dependence on the level of intercell Stokes radiation. When compared with the experimental results of Figs. 3 and 4 there is reasonable agreement with the transient modeling both in the qualitative trends and in the actual data.

Despite the agreement between transient theory and experiment on the bulk parameters of the system (R and A) there is some discrepancy in the degree of modulation present on the intercell radiation. A possible explanation is the presence of nonuniform spatial depletion of the pump beam within the amplifier. Support for this statement is gained by monitoring the temporal evolution of the intercell radiation at one radial position in the beam cross section. Figure 9(a) shows the behavior of the intercell Stokes radiation on axis by recording the transmission of the beam through a 200-μm pinhole. The on-axis radiation displays deep modulation in contrast to the total power integrated over the beam cross section [Fig. 5(b)] and therefore gives considerably better agreement with the simulation of Fig. 9(b).

DISCUSSION

The generator–amplifier system described above has been demonstrated to extend the use of SBS phase-conjugate mirrors to higher powers. In this section, a more detailed consideration of the operation of the system, including its temporal and spatial characteristics, is made.

The physical length and hence round-trip transit time of the two-cell configuration is an important factor affecting its performance. This includes such features as laser-coherence requirement, transient response time of the system, and the system's power-limiting ability.

In order for the two-cell system to attain steady-state behavior with pulsed laser radiation it is necessary for the pulse duration to be long compared with the SBS onset time and intercell transit time (τ). Similarly, for a coher-

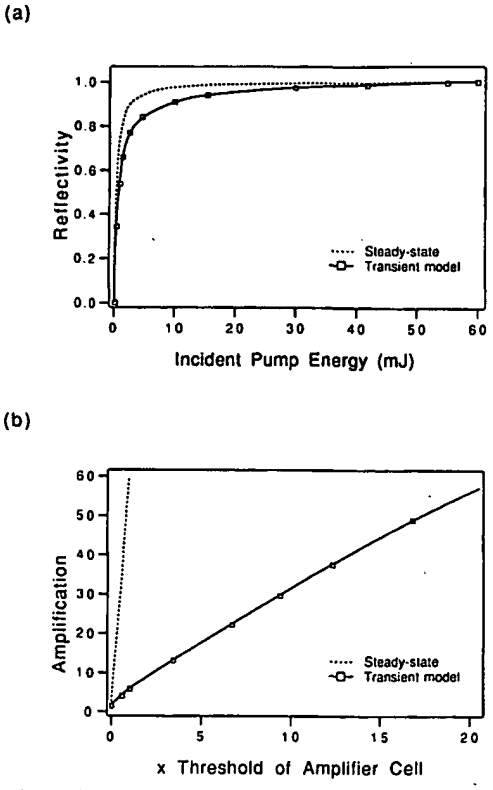

Fig. 8. Transient model and steady-state calculation against energy of (a) energy reflectivity R and (b) energy amplification factor A. Squares denote points where numerical simulations were performed.

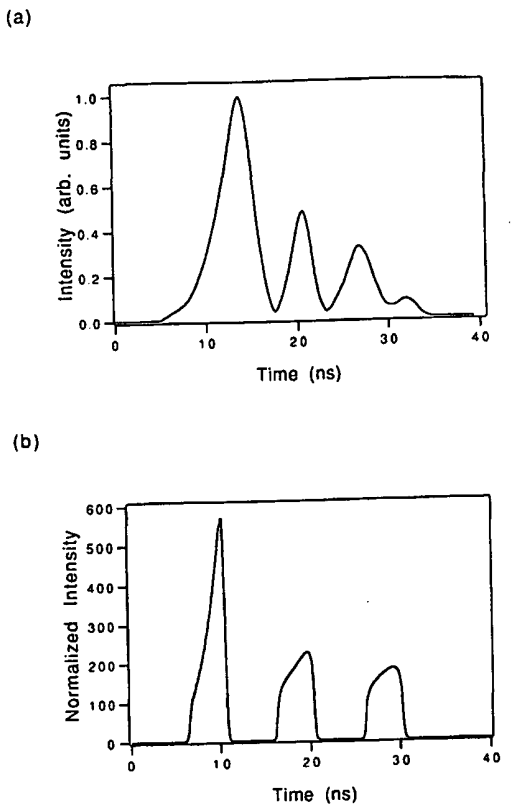

Fig. 9. Temporal profile of the intercell Stokes radiation (a) measured on axis and (b) simulated numerically.

ent interaction it is necessary for the laser-coherence length to be at least twice the total length of the two-cell system (i.e., twice the sum of the cell lengths and intercell separation).

One of the main features of the generator–amplifier arrangement is that once the amplifier is seeded the pump beam undergoes strong depletion, thereby reducing the power transmitted to the generator and so protecting it from damage. If the intercell transit time is long, then there will be a lengthy delay before the amplifier is seeded and power limiting becomes effective. During this time sufficient power could reach the generator cell to result in optical breakdown. For this reason and for others described above, it is desirable to use a relatively compact two-cell geometry.

A further feature demonstrated by the simulations but also observed experimentally at high powers is the ability to achieve greater-than-unity reflectivity on a transient basis. This overshoot by the Stokes radiation can be explained by storage of radiation in the two-cell system. The excess of Stokes power over the input pump will only be temporary since the severe depletion of the pump will reduce the seeding signal, resulting in an overshoot for a time of the order of twice the intercell transit time (2τ). The amount of overshoot is dependent on the gain of the amplifier and on the intercell losses. For low losses, the seeding level can be high, leading to a substantial overshoot. This feature is entirely analogous to that observed in systems using optical feedback.[12] It is also the basis for laser-pulse compression in long-cell Brillouin and Raman schemes.[13–16]

As well as achieving high reflectivities for high input powers, it is important that the two-cell system can also satisfactorily conjugate the pump-beam spatial distribution. The observations made at the end of the previous section are relevant to this issue.

As previously described, the modulation recorded on axis for the intercell radiation was greater than for the total signal integrated over the beam cross section. The same was also true for the intercell radiation recorded 2.1 mm off the beam axis (results not shown here). The only way to reconcile these observations is if a nonuniform spatial depletion of the pump results in a relative temporal delay in the depletion over the beam cross section. The temporal form of the nonuniform spatial depletion occurs owing to the center of the Gaussian (TEM_{00}) beam reaching threshold before the weaker wings and hence experiencing depletion sooner. The presence of this nonuniform depletion did not appear to affect the ability of the two-cell system to phase conjugate Gaussian beams satisfactorily. The reflected Stokes radiation was in the form of a high-quality, low-divergence beam with a negligible uncorrelated noise component. However these spatial-depletion effects may limit the ability to phase conjugate aberrated beams adequately.

The performance of the generator cell could be improved by the introduction of optical feedback, which has been shown to reduce the threshold and increase the phase-conjugate fidelity of the SBS process.[12] The level of pump power that can safely be introduced into the two-cell system can be raised by the use of optical filters between the cells. This technique has the drawback, however, of raising the threshold of the device. An alternative method that avoids this problem has been proposed by previous authors[4] and involves the use of a third Brillouin cell inserted between the amplifier and generator. By selecting a Brillouin medium with a different frequency shift (Ω_B) the cell acts as a nonlinear filter with high transmission at low pump powers and low transmission at high pump powers.

CONCLUSIONS

The results presented in this paper have shown that a two-cell generator–amplifier system is an effective way of obtaining phase conjugation of high-power radiation by the SBS process. Numerical simulations have been presented and shown to provide a reasonable prediction of the transient response of the experimental system. Similarly the steady-state calculations are in agreement with the broad numerical and experimental trends. This technique could be used to scale to even higher laser powers by introducing further cells with progressively decreasing apertures. An alternative would be to use a tapering amplifier cell as has been used in experiments to produce laser-pulse compression.[13–15] A more extensive investigation into the ability of the two-cell system to phase conjugate aberrated beams would reveal the usefulness of the technique in practical applications.

APPENDIX A

When the propagation terms in Eqs. (1a) and (1b) are neglected and the dependent and independent variables are

made dimensionless, the resulting simplified equations are

$$\frac{\partial e}{\partial \eta} = -sq, \tag{A1a}$$

$$\frac{\partial s}{\partial \eta} = -eq, \tag{A1b}$$

$$\frac{\partial q}{\partial \tau} = es - q, \tag{A1c}$$

where $e = E(gL/2)^{1/2}, s = S(gL/2)^{1/2}, q = (gL\Gamma/2)Q$, and the space and time variables are scaled as $\eta = z/L$ and $\tau = \Gamma t$. The SBS interaction as described by Eqs. (A1) still poses a boundary-value problem with pump and Stokes fields specified at opposite ends of the cell [i.e., $e(\eta = 0,\tau)$ and $s(\eta = 1,\tau)$]. The problem can be transformed to an initial-value problem by defining sum and difference variables as follows:

$$\lambda_1(\tau)u(\eta,\tau) = e(\eta,\tau) + s(\eta,\tau), \tag{A2a}$$

$$\lambda_2(\tau)v(\eta,\tau) = e(\eta,\tau) - s(\eta,\tau), \tag{A2b}$$

which yields a new set of equations:

$$\frac{\partial u}{\partial \eta} = -uq, \tag{A3a}$$

$$\frac{\partial v}{\partial \eta} = +vq, \tag{A3b}$$

$$\frac{\partial q}{\partial \tau} = es - q, \tag{A3c}$$

with

$$e = \frac{1}{2}(\lambda_1 u + \lambda_2 v), \qquad s = \frac{1}{2}(\lambda_1 u - \lambda_2 v). \tag{A4}$$

The presence of the multipliers λ_1 and λ_2 permits the values of the variables u and v to be specified at one value of η. A good choice is to select the position $\eta = 0$ and assign $u(0,\tau) = 1$ and $v(0,\tau) = 1$.

When the above values are substituted into the boundary conditions in terms of the new variables the result is

$$\frac{1}{2}[\lambda_1(\tau) + \lambda_2(\tau)] = e(0,\tau), \tag{A5a}$$

$$\frac{1}{2}[\lambda_1(\tau)u(1,\tau) - \lambda_2(\tau)v(1,\tau)] = \frac{1}{2}[\lambda_1(\tau)u(1,\tau) + \lambda_2(\tau)v(1,\tau)]\exp\left(-\frac{D}{2}\right), \tag{A5b}$$

which can be solved simultaneously for $\lambda_1(\tau)$ and $\lambda_2(\tau)$ when Eqs. (A3a) and (A3b) have been integrated to yield $u(1,\tau)$ and $v(1,\tau)$. Substituting for $\lambda_1(\tau)$ and $\lambda_2(\tau)$ in Eqs. (A4) then allows the values for the fields e and s to be calculated. The process is repeated for each time step in the simulation and enables Eqs. (A1) to be modeled as closely as the numerical algorithm allows.

ACKNOWLEDGMENTS

The authors acknowledge financial support from the Royal Armament Research and Development Establishment (RARDE), Fort Halstead. G. J. Crofts thanks the RARDE for support in the form of a Cooperative Awards in Science and Engineering studentship.

REFERENCES

1. B. Ya Zel'dovich, N. F. Pilipetsky, and V. V. Shkunov, *Principles of Phase Conjugation*, Vol. 42 of Springer Series in Optical Sciences (Springer, New York, 1985), Chap. 4.
2. D. R. Hull, R. A. Lamb, and J. R. Digman, "Efficient phase conjugation at high energies using two cells," Opt. Commun. **72**, 104–108 (1989).
3. N. G. Basov, V. F. Efimkov, I. G. Zubarev, A. V. Kotov, and S. I. Mikhailov, "Control of the characteristics of reversing mirrors in the amplification regime," Sov. J. Quantum Electron. **11**, 1335–1337 (1981).
4. A. F. Vasil'ev and V. E. Yashin, "Stimulated Brillouin scattering at high values of the excess of the pump energy above the threshold," Sov. J. Quantum Electron. **17**, 644–647 (1987).
5. V. N. Alekseev, V. V. Golubev, D. I. Dmitriev, A. N. Zhilin, V. V. Lyubimov, A. A. Mak, V. I. Reshetnikov, V. S. Sirazetdinov, and A. D. Starikov, "Investigation of wavefront reversal in a phosphate glass laser amplifier with a 12 cm aperture," Sov. J. Quantum Electron. **17**, 455–458 (1987).
6. D. A. Glazkov, V. F. Efimkov, I. G. Zubarev, S. A. Pastukhov, and V. B. Sobolev, "Competition between Stokes waves in a phase-conjugating hypersonic mirror based on an oscillator–amplifier system operating under saturation conditions," Sov. J. Quantum Electron. **18**, 974–977 (1988).
7. I. A. Varlamova, V. V. Golubev, and V. S. Sirazetdinov, "Investigation of oscillator amplifier phase-conjugating mirrors based on stimulated Brillouin scattering," Sov. J. Quantum Electron. **19**, 1631–1634 (1989).
8. R. A. Mullen, D. J. Vickers, and D. M. Pepper, "Stimulated photorefractive scattering phase conjugators backseeded with retroreflector arrays," in *Digest of Conference on Lasers and Electro-Optics* (Optical Society of America, Washington, D.C., 1990), paper CTU D3.
9. G. J. Crofts and M. J. Damzen, "Steady-state analysis and design criteria of two-cell stimulated Brillouin scattering systems," Opt. Commun. **81**, 237–241 (1991).
10. E. L. Bubis, L. R. Konchalina, and A. A. Shilov, "Influence of thermal self-interaction on phase conjugation of laser radiation by the stimulated Brillouin scattering in liquids at high values of the excess above the power threshold," Sov. J. Quantum Electron. **19**, 925–927 (1989).
11. A. I. Erokhin, V. I. Kovalev, and F. S. Faizullov, "Determination of the parameters of a nonlinear response of liquids in an acoustic resonance region by the method of non-degenerate four-wave interaction," Sov. J. Quantum Electron. **16**, 872–877 (1986).
12. G. K. N. Wong and M. J. Damzen, "Investigations of optical feedback used to enhance stimulated scattering," IEEE J. Quantum Electron. **26**, 139–148 (1990).
13. D. T. Hon, "Pulse compression by stimulated Brillouin scattering," Opt. Lett. **5**, 516–518 (1980).
14. M. J. Damzen and M. H. R. Hutchinson, "Laser pulse compression by stimulated Brillouin scattering in tapered waveguides," IEEE J. Quantum Electron. **QE-19**, 7–14 (1983).
15. M. J. Damzen and M. H. R. Hutchinson, "High-efficiency laser-pulse compression by stimulated Brillouin scattering," Opt. Lett. **8**, 313–315 (1983).
16. J. R. Murray, J. Goldhar, D. Eimerl, and A. Szöke, "Raman pulse compression of excimer lasers for application to laser fusion," IEEE J. Quantum Electron. **QE-15**, 342–368 (1979).